



Multivariate Pattern Analysis of Electroencephalography Data in a Demand-Selection Task

David López-García¹, Alberto Sobrado¹, J. M. González-Peñalver¹,
Juan Manuel Górriz², and María Ruz¹(✉)

¹ Mind, Brain and Behavior Research Center (CIMCYC),
University of Granada, Granada, Spain
{[dlopez](mailto:dlopez@ugr.es), [mruz](mailto:mruz@ugr.es)}@ugr.es

² Signal Theory, Telematics and Communications Department (TSTC),
University of Granada, Granada, Spain
gorriz@ugr.es

Abstract. Cognitive effort is costly and partly aversive, and thus humans usually avoid it if given the chance. In Demand-Selection Tasks (DST), participants tend to choose the easy option over the hard one. The neural underpinnings of this effect, however, are not well understood. The current study is an initial approximation to adapt a DST to a format that allows measuring concurrent high-density electroencephalography. We used multivariate pattern analysis (MVPA) to decode conflict-related neural processes associated with congruent or incongruent events in a time-frequency resolved way and determined how different frequency bands contribute to the overall decoding accuracy. The decoding analysis involved the use of Support Vector Machines, a supervised learning algorithm that provides a theoretically elegant, computationally efficient, and very effective solution for many practical pattern recognition problems. Preliminary results show significant differences in activation patterns for congruent and incongruent trials, yielding 80% of decoding accuracy 400 ms after the stimulus onset. The results of frequency bands contribution analysis suggest that context-dependent proportion of congruency effect may rely on neural processes operating in Delta and Theta-band frequencies.

Keywords: Multivariate pattern analysis · Electroencephalography · Classification · Support Vector Machine · Demand-Selection Task

1 Introduction

Cognitive effort is costly and partly aversive, and thus humans usually avoid it if given the chance. In Demand-Selection Tasks (DST)[1], participants tend to choose the easy option over the hard one. The neural underpinnings of this effect, however, are not well understood. The current study is an initial approximation to adapt a DST to a format that allows measuring concurrent high-density

electroencephalography. Supervised machine learning algorithms, more specifically Support Vector Machines (Vapnik, 1979), in conjunction with several neuroimaging techniques, such as functional Magnetic Resonance Imaging (fMRI), Electroencephalography (EEG) or Magnetoencephalography (MEG), have been widely and successfully applied in clinical applications, such as computer-aided diagnosis of Alzheimer’s disease [2–5], automatic sleep stages classification [6, 7] or automatic detection of sleep disorders [8]. Recently, these techniques are gaining popularity in Cognitive Neuroscience, especially in fMRI studies. However, the poor temporal resolution of the fMRI signal prevents an accurate time-resolved study of the cognitive processes. For this reason, the use of these techniques is spreading and they are being applied to M/EEG signals, studying the neural dynamics of face detection [9], the process of memory retrieval [10], the representational dynamics of task and object processing in humans [11] or decoding spoken words in bilingual listeners [12].

This study uses multivariate pattern analysis (MVPA) to decode conflict-related neural processes associated to congruent or incongruent events in a time-frequency resolved way. Due to the noisy nature of the EEG signal, a trial averaging approach has been carried out during the feature extraction stage, increasing the signal-to-noise ratio (SNR). In addition, we determined how different frequency bands contribute to the overall decoding accuracy, showing that context-dependent proportion of congruency effect may rely on neural processes operating in Delta and Theta frequency bands [13].

2 Materials and Methods

Participants. Thirty-two healthy individuals (21 females, 29 right-handed, mean age = 24.65, SD = 4.57) were recruited for the experiment. Subjects had normal or corrected-to-normal vision and none reported any neurological or psychiatric disorder. All of them provided informed, written consent before the beginning of the experiment and received a 10-euro payment or course credits in exchange for their participation. The experiment was approved by the Ethics Committee of the University of Granada.

Experimental Setup. Stimuli presentation and behavioral data collection were carried out using MATLAB (MathWorks) in conjunction with Psychtoolbox-3 Toolbox [14], in a magnetically shielded room. The visual stimuli were presented in an LCD screen (Benq, 1920 × 1080 resolution, 60 Hz refresh rate) and placed 68.31 ± 5.37 cm away of subject’s Glabella. Using a photodetector, the stimuli onset lag was measured at 8 ms, which corresponds to half of the refresh rate of the monitor. Triggers were sent from the presentation computer to the EEG recording system through an 8-bit parallel port and using a custom MATLAB function in conjunction with inpoutx64 driver [15].

Stimuli. The predictive cue acted as a difficulty selector, and consisted of two squares of different colors stacked and presented in the center of the screen (visual angle $\sim 5^\circ$). In forced blocks, a small white indicator (circle 50% or

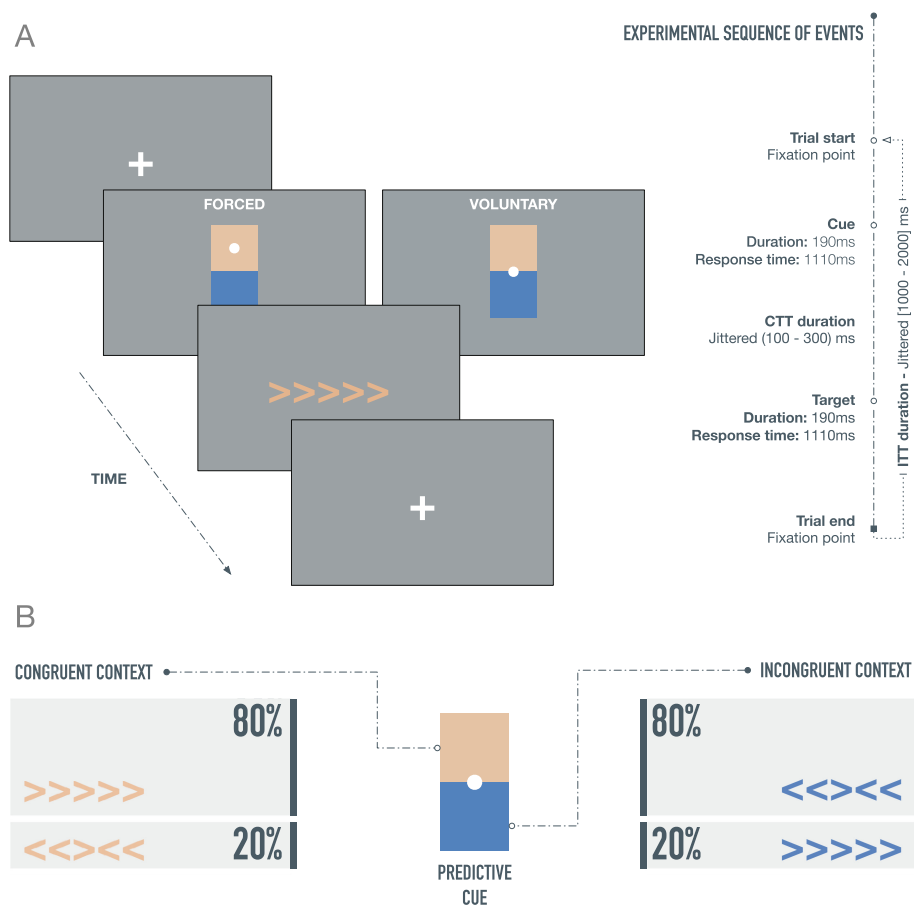


Fig. 1. (A) Experimental sequence of events in case of a correct response on both cue and stimulus flanker. A trial starts with a fixation point, followed by a cue, which acts as a color picker. Subjects have to choose (freely or forced, depending on the block type) the possible color of the upcoming target stimulus. Finally, after a variable time interval (100–300 ms) the target stimulus appears and subjects have to respond accordingly to the orientation of the central arrow. Another variable time interval started before the beginning of the next trial. The cue and the target stimulus remained in the screen for 190 ms. (B) Cognitive effort manipulation through the percentage of congruent and incongruent trials. Each cue color is associated to a high and low conflict context. (Color figure online)

square 50%) appeared on top of the color that had to be chosen. In voluntary blocks, this indicator appeared between the two colored squares (see Fig. 1). Each target stimulus consisted of five arrows pointing left or rightwards, which were displayed at the center of the screen (visual angle $\sim 6^\circ$). The color of the target stimulus depended on the previously selected color.

Experimental Design. The Color-Based Demand-Selection Task [Fig. 1 (a)], modified from [1], consisted of a cue-target sequence where participants were required to choose (voluntarily or forced, in different blocks: 4 blocks, 240 trials per block, ~ 90 min) the color of the upcoming stimulus and discriminate the orientation (right or left) of an arrow target surrounded by arrows pointing at the same (compatible distracters) or opposite (incompatible distracters) direction. Difficulty, or cognitive effort, was manipulated through the percentage of congruent or incongruent trials associated with each color.

Participants were instructed to respond as fast and accurately as possible, and to not choose color based on personal preference. They were unaware of the cognitive effort manipulation. In order to preserve the signals as clean as possible and remove the least number of trials, participants were encouraged to remain as still and relaxed as possible, avoiding face muscle activity and eye movements, but blinking normally. The order of the blocks, cue colors, response keys and color-conflict context mappings were counterbalanced between subjects.

Behavioral Data Acquisition and Preprocessing. The reaction time (RT) and error rates were registered for each subject. Before the statistical analysis, the first trial of each block, trials with choice errors and trials after errors were filtered out, as suggested in [16]. Finally, RT outliers were also rejected using a ± 2.5 SD threshold, calculated individually per subject. As a result, there was a total removal of 19% of the trials.

EEG Data Acquisition and Preprocessing. High-density electroencephalography was recorded from 65 electrodes mounted on an elastic cap (actiCap slim,

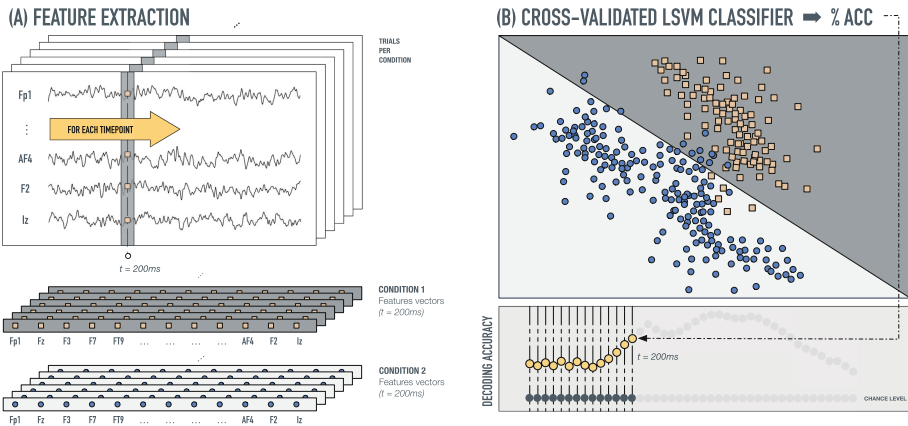


Fig. 2. (A) Feature extraction process in simulated data. The feature vectors of each condition and time point consisted of an z-scored voltage array for all the scalp electrodes. For an improved SNR, five trials were averaged before the feature extraction. (B) Cross-validated LSVM classifier. For each time point, a LSVM was trained and tested (stratified k-fold cross-validation, $k = 10$). Chance level was calculated permuting the labels.

Brain Products). The TP9 and TP10 electrodes were used to record the electrooculogram (EOG) and were placed below and next to the left eye of the subject. Impedances were kept below 5 k. EEG activity was referenced to the FCz electrode and signals were digitalized at a sampling rate of 1 KHz.

Electroencephalography recordings were average referenced, downsampled to 256 Hz, and digitally filtered using a bandpass FIR filter [0.5–40 Hz], preserving the phase information. No channel was interpolated for any subject. EEG recordings were epoched [−1000, 2000 ms centered at the target arrows] and baseline corrected [−200, 0 ms], extracting data only from correct trials. A total of 90 518 epochs (target, cue and cue response) were extracted. To remove blinks from the remaining data, Independent Component Analysis (ICA) was computed using the *runica* algorithm from EEGLAB [17], excluding TP9 and TP10 channels. Artifactual components were rejected by visual inspection of raw activity of each component, scalp maps and power spectrum. Then, an automatic trial rejection process was performed, pruning the data from no stereotypical artifacts. The trial rejection procedure was based on (1) extreme values: all trials with amplitudes in any electrode out of $\pm 75\mu\text{V}$ range were automatically rejected ($\sim 7\%$ of the total sample); (2) abnormal spectra: the spectrum should not deviate from baseline by $\pm 50\text{ dB}$ in the 0–2 Hz frequency window (which is optimal for localizing any remaining eye movements) and should not deviate by -100 dB or $+25\text{ dB}$ in 20–40 Hz (useful for detecting muscle activity) ($< 1\%$ of the total sample).

Multivariate Pattern Analysis (MVPA). The MVPA for the decoding analysis was performed in MATLAB by a custom-developed set of linear Support Vector Machines (LSVM), trained to discriminate between congruent and incongruent target stimuli. To avoid skewed classification results due to a possible unbalanced dataset, the prior probabilities of each class were set to uniform. The rest of the classification parameters remained by default. The generalization performance of the classifiers was calculated through cross-validation technique (stratified k-fold, $k = 10$).

To obtain the classification performance in a time-resolved way, the feature vectors were extracted as shown in Fig. 2. Thus, the classification procedure, for each subject, ran as follows: (1) For each timepoint and trial, we generated two feature vectors (one for each condition or class) consisting of the raw potential measured in all electrodes (excluding EOG electrodes: TP9 and TP10). (2) Features vector containing raw potential values were normalized (z-score). (3) LSVMs were trained and cross-validated, resulting in a single value of accuracy for each timepoint and subject. (4) Finally, a single measure of accuracy for each timepoint was calculated by averaging the classification performance over all the subjects. The chance level was calculated following the former analysis but using randomly permuted labels for each trial.

In a second analysis, to increase the signal-to-noise ratio [18] (SNR), improving the overall decoding performance and reducing the computational load, each subjects dataset was reduced by randomly averaging a number of trials belonging to the same condition. The number of trials to average is a trade-off between

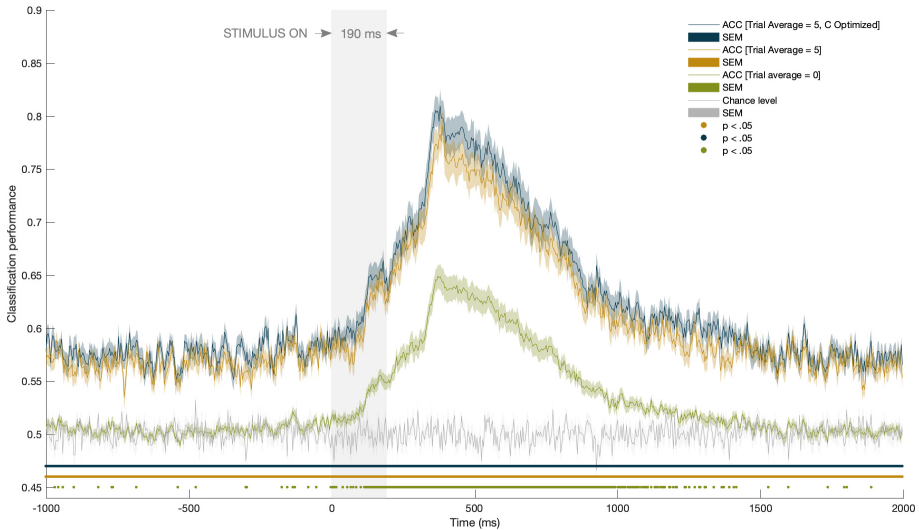


Fig. 3. Classification performance. The green line represents the classification results when no trial average was carried out. An improved classification performance is shown in orange, averaging 5 trials before the feature extraction. Finally, the former analysis was repeated optimizing the cost parameter C (fivefold cross-validated), shown in blue. The gray line represents the classifier chance level, calculated through permuted labels. The shaded areas show the standard error. The statistically significant regions are indicated on the bottom of the figure by colored dots. (Color figure online)

an increased classification performance (due to an increased SNR) and the variance in the classifier performance, since reducing the trial per condition typically increases the variance in (within-subject) classifier performance [19]. The optimal number of trials to average depends on the data. In our dataset (~ 500 trials per condition and subject) considering that averaging more trials does not increment the decoding performance linearly, we found that averaging 5 trials is a good trade-off between SNR and trials per conditions (~ 100 trials per condition and subject). Finally, a search-grid based cost parameter (C) optimization was carried out using fivefold cross-validation on the training set and increasing the final decoding accuracy.

Frequency Contribution Analysis. The contribution of each frequency band to the overall decoding accuracy was assessed through a sliding filter approach. We designed a band-stop FIR filter (4 Hz bandwidth, 0.5 Hz transition band, 2816 filter order, Blackman window) and pre-filtered the EEG data (37 overlapped frequency bands, between 2–40 Hz and logarithmically spaced steps) producing 37 filtered versions of the original EEG dataset. The former decoding analysis was repeated for each filtered version and the importance of each filtered-out band was quantified computing the difference in decoding accuracy between the filtered and the original datasets.

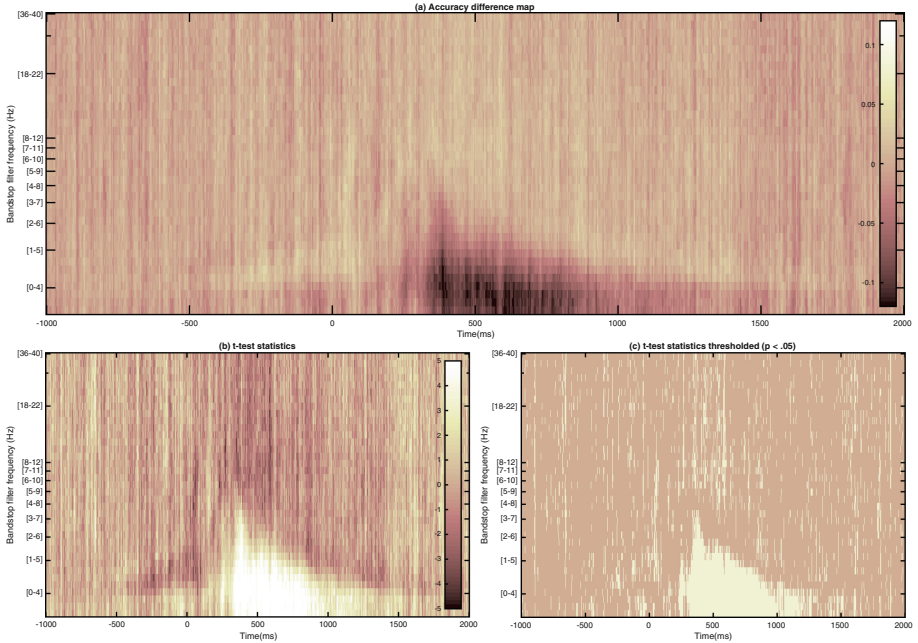


Fig. 4. Frequency contribution analysis. (A) Classification differences when a specific frequency band is filtered-out. (B) T-test statistics showing significant differences in classification at each time point and frequency band. (C) $p < .05$ thresholded significance map.

3 Results and Discussion

The behavioral results replicate well-known conflict effects linked to context-dependence congruency. Effort avoidance was observed in voluntary decision blocks (percentage of choice of easy 57.11% SEM=2.93 vs difficult 42.88% SEM=2.93 contexts; $t = 2.42$, $p = .021$). Planned comparisons show significant differences in reaction time between contexts for both congruent ($F(1,31) = 12.76$, $p = .001$, $\eta_p^2 = .292$) and incongruent trials ($F(1,31) = 10.72$, $p = .003$, $\eta_p^2 = .257$) and interaction of context and congruency, showing the context-dependent congruency effect.

The electrophysiological analyses (Fig. 3) show significant differences ($p < 0.05$) in activation patterns for congruent and incongruent trials, peaking 400 ms after the stimulus onset. A paired t-test was computed comparing the classification performance mean at each time point with the classifier chance level, which was calculated through permuted labels. The significant region extends from stimulus onset ($t = 0$ ms) to 1500 ms later, when no trial average was carried out. When the signal to noise ratio was increased by trial averaging, this significant region extends throughout the entire analyzed temporal window, which suggests that neural patterns associated to congruent or incongruent tri-

als are significantly different even before the stimulus presentation. These results are reasonable, since the stimulus onset is preceded by a predictive cue, which indicates with 80% of validity, once the context is chosen (easy or hard), if the following trial will be congruent or incongruent. These activation patterns differences between conditions may rely on the differences in preparatory neural mechanisms triggered by the selected context, reasserting the context-dependent congruency effects in reaction times showed in the behavioral results.

A sliding bandstop filter approach was followed to study the contribution of each frequency band to the overall decoding accuracy, showing that context-dependent proportion of congruency effect may rely on neural processes operating in Delta and Theta frequency bands. Figure 4A shows how decoding accuracy significantly drops when frequencies up to 8 Hz were filtered-out. A paired t-test was computed comparing the classification performance mean at each time point and frequency band with the classifier performance when no frequency was filtered-out (Fig. 4B). Finally, Fig. 4C shows a thresholded significance map ($p < 0.05$) of the former analysis.

4 Conclusion

The current study is an initial approximation to adapt a DST to a format that allows measuring concurrent high-density electroencephalography. We used multivariate pattern analysis (MVPA) to decode conflict-related neural processes associated with congruent or incongruent events in a time-frequency resolved way, yielding 80% of decoding accuracy 400 ms after the stimulus onset. Our preliminary results of frequency bands contribution analysis suggest that context-dependent proportion of congruency effect may rely on neural processes operating in Delta and Theta-band frequencies. For a better understanding of preparation processes and conflict effects, it would be of interest to continue analyzing our data, focusing not only on the target stimulus, but also on the cue. Further detailed analyses should be carried out to study the activation differences between forced and voluntary blocks or high and low congruency contexts.

Acknowledgments. This research was supported by the Spanish Ministry of Economy and Business under the TEC2015-64718-R and PSI2016-78236-P projects. The first author of this work is supported by a grant from the Spanish Ministry of Economy and Business (BES-2017-079769).

References

1. Kool, W., McGuire, J.T., Rosen, Z.B., Botvinick, M.M.: Decision making and the avoidance of cognitive demand. *J. Exp. Psychol.: Gen.* **139**(4), 665 (2010)
2. Ramírez, J., et al.: Computer-aided diagnosis of Alzheimer's type dementia combining support vector machines and discriminant set of features. *Inf. Sci.* **237**, 59–72 (2013)

3. Chaves, R., et al.: SVM-based computer-aided diagnosis of the Alzheimer's disease using t-test nmse feature selection with feature correlation weighting. *Neurosci. Lett.* **461**(3), 293–297 (2009)
4. Salas-Gonzalez, D., et al.: Computer-aided diagnosis of Alzheimer's disease using support vector machines and classification trees. *Phys. Med. Biol.* **55**(10), 2807 (2010)
5. Álvarez, I., et al.: Alzheimer's diagnosis using eigenbrains and support vector machines. *Electron. Lett.* **45**(7), 342–343 (2009)
6. Koley, B., Dey, D.: An ensemble system for automatic sleep stage classification using single channel EEG signal. *Comput. Biol. Med.* **42**(12), 1186–1195 (2012)
7. Aboalayon, K.A.I., Ocbagabir, H.T., Faezipour, M.: Efficient sleep stage classification based on EEG signals. In: *IEEE Long Island Systems, Applications and Technology (LISAT) Conference 2014*, pp. 1–6. IEEE (2014)
8. López-García, D., Ruz, M., de Inestrosa, J.R.P., Sáez, J.M.G.: Automatic detection of sleep disorders: multi-class automatic classification algorithms based on support vector machines. In: *International Conference on Time Series and Forecasting (ITISE 2018)*, vol. 3, pp. 1270–1280 (2018)
9. Cauchoix, M., Barragan-Jason, G., Serre, T., Barbeau, E.J.: The neural dynamics of face detection in the wild revealed by MVPA. *J. Neurosci.* **34**(3), 846–854 (2014)
10. Kerrén, C., Linde-Domingo, J., Hanslmayr, S., Wimber, M.: An optimal oscillatory phase for pattern reactivation during memory retrieval. *Curr. Biol.* **28**(21), 3383–3392 (2018)
11. Hebart, M.N., Bankson, B.B., Harel, A., Baker, C.I., Cichy, R.M.: The representational dynamics of task and object processing in humans. *Elife* **7**, e32816 (2018)
12. Correia, J.M., Jansma, B., Hausfeld, L., Kikkert, S., Bonte, M.: EEG decoding of spoken words in bilingual listeners: from words to language invariant semantic-conceptual representations. *Front. Psychol.* **6**, 71 (2015)
13. Cohen, M.X., Donner, T.H.: Midfrontal conflict-related theta-band power reflects neural oscillations that predict behavior. *Am. J. Physiol.-Heart Circ. Physiol.* **110**, 2752–2763 (2013)
14. Kleiner, M., Brainard, D., Pelli, D., Ingling, A., Murray, R., Broussard, C., et al.: What's new in psychtoolbox-3. *Perception* **36**(14), 1 (2007)
15. Logix4U, Gibbons, P.: Inpout32 is an open source windows DLL and driver to give direct access to hardware ports
16. Schouppe, N., Demanet, J., Boehler, C.N., Ridderinkhof, K.R., Notebaert, W.: The role of the striatum in effort-based decision-making in the absence of reward. *J. Neurosci.* **34**(6), 2148–2154 (2014)
17. Delorme, A., Makeig, S.: EEGLAB: an open source toolbox for analysis of single-trial EEG dynamics including independent component analysis. *J. Neurosci. Methods* **134**(1), 9–21 (2004)
18. Isik, L., Meyers, E.M., Leibo, J.Z., Poggio, T.A.: The dynamics of invariant object recognition in the human visual system. *Am. J. Physiol.-Heart Circ. Physiol.* **111**, 91–102 (2013)
19. Grootswagers, T., Wardle, S.G., Carlson, T.A.: Decoding dynamic brain patterns from evoked responses: a tutorial on multivariate pattern analysis applied to time series neuroimaging data. *J. Cogn. Neurosci.* **29**(4), 677–697 (2017)